BIOCHEMISTRY
including biophysical chemistry & molecular biology

Accelerated Publication

pubs.acs.org/biochemistry

Human Translation Initiation Factor eIF4G1 Possesses a Low-Affinity ATP Binding Site Facing the ATP-Binding Cleft of eIF4A in the eIF4G/eIF4A Complex

Sabine R. Akabayov,[†] Barak Akabayov,[†,‡] and Gerhard Wagner[†,*]

[†]Department of Biological Chemistry and Molecular Pharmacology, Harvard Medical School, Longwood Avenue, Boston, Massachusetts 02115, United States

[‡]Department of Chemistry, Ben-Gurion University of the Negev, Be'er-Sheva 84105, Israel

Supporting Information

ABSTRACT: Eukaryotic translation initiation factor 4G (eIF4G) plays a crucial role in translation initiation, serving as a scaffolding protein binding several other initiation factors, other proteins, and RNA. Binding of eIF4G to the ATP-dependent RNA helicase eukaryotic translation initiation factor 4A (eIF4A) enhances the activity of eIF4A in solution and in crowded environments. Previously, this activity enhancement was solely attributed to eIF4G, conferring a closed, active conformation upon eIF4A. Here we show that eIF4G contains a low-affinity binding site at the entrance to the ATP-binding cleft on eIF4A, suggesting that regulation of the local ATP concentration may be an additional reason for the enhancement in activity.

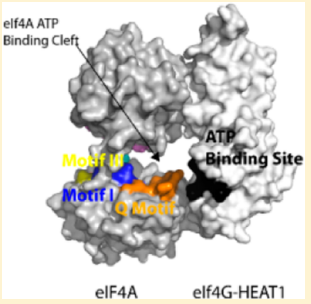

The control of translation (mRNA-encoded protein synthesis) is crucial for cell proliferation and differentiation. More than 10 eukaryotic translation initiation factors are known to be involved in the assembly of the 80S ribosome/RNA complex, allowing placement of the initiator Met-tRNA at the correct start codon of the mRNA.[1] The dominant mechanism used by cellular mRNAs, named cap-dependent translation, requires the recognition of the 5′ m7G cap structure of the mRNA by the cap binding complex eIF4F. The eIF4F complex is composed of cap-binding subunit eIF4E, RNA helicase eukaryotic translation initiation factor 4A (eIF4A), and scaffolding protein eukaryotic translation initiation factor 4G (eIF4G).[2−4] Eukaryotic translation factor 4A (eIF4A) is the prototypic member of the DEAD-box family of RNA helicases,[5] a subfamily of superfamily 2 (SF2) of RNA helicases.[6] ATP-dependent RNA helicase eIF4A unwinds secondary structure in the 5′ untranslated region (UTR) of mRNAs to facilitate 40S ribosome binding and scanning for the start codon. eIF4A by itself is a poor ATPase and helicase (k_{cat} = 3 min^{-1}).[7] However, these activities are stimulated when eIF4A is part of a multiprotein complex including eIF4G, eIF4E, eIF4B, and/or eIF4H.[8−12]

eIF4G plays a crucial role in translation initiation, serving as a scaffolding protein that binds several initiation factors (the cap-binding protein eIF4E, the RNA helicase eIF4A, and eIF3) and other proteins [poly(A)-binding protein, eIF4E kinase, and Mnk]. Human eIF4G contains three HEAT repeat domains in the C-terminal two-thirds of its sequence. The first two, HEAT1 and HEAT2, contain binding sites for the ATP-dependent RNA helicase eIF4A. It has been shown that the interaction with HEAT1 enhances the activity of eIF4A by 4-fold in solution.[13]

In solution, eIF4A exists in a flexible, open conformation. eIf4G-HEAT1 forms a soft clamp conferring a closed conformation upon eIF4A. The enhancement in activity was generally attributed to this change from the open to the closed, active conformation.[14] Assuming the only reason for the enhancement in activity stems from the binding of eIF4G and the accompanying change to the closed conformation, no additional enhancement would be expected once eIf4A is in the closed conformation. We have recently shown that macromolecular crowding shifts the equilibrium toward the closed, active conformation of eIF4A. However, additional enhancement of eIF4A activity is observed in the presence of eIf4G-HEAT1.[15] This additional enhancement suggests that the conformational change is not the only reason for the increase in activity.

The crystal structure of eIF4GII-HEAT1 was determined using X-ray crystallography; however, the structure of a 40-residue loop was not resolved.[16] The structure of free yeast eIF4A was successfully determined,[17] but no structure for free full length human eIF4A is available. The two recA-like domains are very similar among the DEAD-box helicases; however, the interdomain angle varies greatly. A structure of the closed conformation of human eIF4A in complex with PCDC4 is available[18] and is very similar to the structure of yeast eIF4A in complex with yeast eIF4GII-HEAT1.[19] We

Received: May 18, 2014
Revised: September 25, 2014
Published: September 25, 2014

   dx.doi.org/10.1021/bi500600m | *Biochemistry* 2014, 53, 6422−6425

recently reported the low-resolution structures of human eIF4A and its complex with eIF4G1-HEAT1 in buffer and a crowded environment showing a significant structural difference.[15]

Here we report the discovery of a low-affinity ATP binding site on eIF4GI-HEAT1 that is located just opposite the ATP-binding cleft of eif4A. The sequence of this binding site does not resemble any known ATP binding sites, which have much higher binding affinities. This low-affinity ATP binding site might play a role in the enhancement of eIF4A activity by regulating local ATP concentrations.

eIF4G-HEAT1 was expressed and purified as described previously.[20] ^{15}N- and D-labeled eIF4G-HEAT1 was expressed in minimal medium. ATP was purchased from Roche Molecular Biochemicals. Poly(U) was purchased from Dharmacon. For nuclear magnetic resonance (NMR) samples, the ^{15}N- and D-labeled protein was concentrated using Millipore (Bedford, MA) Centricons to a final concentration of 0.4 mM in a buffer consisting of 10 mM sodium phosphate (pH 6.5), 150 mM NaCl, 20 mM $MgCl_2$, 2 mM DTT, and 0.5 mM EDTA with increasing concentrations of ATP at ATP:eIF4G-HEAT1 ratios of 0:1, 1:1, 15:1, and 25:1, with increasing poly(U) concentrations at poly(U):eIF4G-HEAT1 ratios of 0:1, 0.5:1, 1:1, and 3:1, or with a poly(U):ATP:eif4G-HEAT1 ratio of 15:1:1. ^{15}N TROSY-HSQC spectra were recorded at 298 K on a Bruker Avance DRX 600 MHz spectrometer equipped with a TCI cryoprobe with a Z gradient and processed using NMRPipe[21] and NMRViewJ.[22] The dimensions were set to 2048 (^{1}H) and 400 (^{15}N) points, respectively, corresponding to spectral widths of 12 (^{1}H) and 32 (^{15}N) ppm, respectively. eIF4G-HEAT1 backbone assignment was performed as described previously.[20] Unlabeled protein samples for X-ray absorption near edge spectroscopy (XANES) were concentrated to final concentrations of 0.3−0.7 mM. Each sample contained 300 μM $MnCl_2$ and ATP in a buffer consisting of 20 mM MES (pH 6.5), 150 mM NaCl, 2 mM DTT, 10% glycerol, and increasing concentrations of eIF4G-HEAT1 (0, 0.3, 0.5, and 0.7 mM). The sample components were mixed at ~0 °C and immediately frozen in copper sample holders (10 mm × 5 mm × 0.5 mm) covered with Mylar using liquid nitrogen. XANES data were collected at the National Synchroton Light Source at beamline X3B of Brookhaven National Laboratory. Spectra were recorded as described previously.[23,24] Examination of the samples for visual signs of photoreduction after each scan and sodium dodecyl sulfate−polyacrylamide gel electrophoresis gels after exposure revealed no signs of burn marks, radiation damage, or protein degradation. Data were processed as described previously using Athena X-ray absorption spectroscopy (XAS) data analysis software.[25]

We recorded ^{15}N−^{1}H TROSY-HSQC spectra of [^{15}N,D]-eIf4G-HEAT1 with increasing concentrations of ATP with ATP:eIF4G-HEAT ratios from 0:1 to 25:1 to determine whether ATP binds to eIF4G-HEAT1. The overlay of these spectra for selected residues is shown in Figure 1a. The entire spectrum is shown in Figure S1 of the Supporting Information. Several peaks shifted upon addition of ATP, indicating a binding event. Plotting the changes in chemical shifts versus residue number (Figure S4 of the Supporting Information) and mapping these changes on the structural model of eIF4G-HEAT1 (Figure S5 of the Supporting Information) reveal a contiguous binding site in the N-terminal region, including residues L926, K927, H929, D930, and E931. To confirm that Mg-ATP is the binding partner and not just Mg^{2+}, we measured TROSY-HSQC spectra of eIF4G-HEAT1 alone, with Mg^{2+}

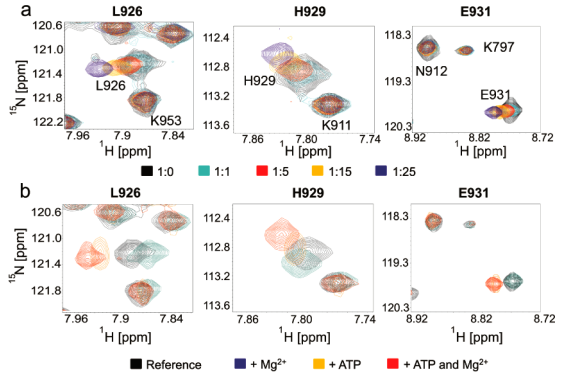

Figure 1. Binding of ATP to eIF4G-HEAT1 as determined by NMR. (a) Titration of ATP to 4GH1 monitored by ^{1}H−^{15}N TROSY-HSQC spectra. The eIF4G-HEAT1:ATP ratio varied from 1:0 to 1:25 as indicated by the color coding in the legend and shown for excerpts for selected residues showing large chemical shift changes upon addition of ATP. The full spectrum is shown in Figure S1 of the Supporting Information. (b) Overlay of ^{15}N TROSY-HSQC spectra of eIF4G-HEAT (black), eIF4G-HEAT with Mg^{2+} (blue), eIF4G-HEAT1 with ATP (orange), and eIF4G-HEAT1 with Mg^{2+} and ATP (red).

only, with ATP alone, and with Mg^{2+} and ATP (Figure 1b). Residues L926 and H929 show chemical shift changes after addition of Mg^{2+} alone and ATP alone and an additional shift for the combination of Mg^{2+} and ATP. These chages in chemical shifts would suggest that both Mg^{2+} and ATP can bind alone to eIF4G-HEAT but that binding of Mg-ATP leads to a change in chemical shift greater than that of either alone. Residue 931 does not show a chemical shift change after addition of Mg^{2+} alone, however, but shows the same change for either ATP alone or Mg-ATP. This would suggest that binding to E931 is not mediated by Mg^{2+} as was observed for the other two residues. Figure S2 of the Supporting Information shows the plot of chemical shift change versus ATP concentration for residues showing the largest chemical shift changes as well as other residues with little or no change for comparison. This graph illustrates clearly that the binding site is a low-affinity binding site as the curve does not show saturation even at high ATP concentrations.

As the observed chemical shift changes are relatively small, we used X-ray absorption near edge spectroscopy (XANES) as an independent method to confirm binding of ATP to eIF4G-HEAT1. XAS utilizes the photoelectric effect in which an X-ray is absorbed and a core level electron is promoted out of the atom. If the energy of the incident X-ray is equal to that of the binding energy of a core level electron, the absorption energy increases significantly. This increase in absorption is called the absorption edge. The energy at which the edge occurs varies on the basis of several characteristics such as the oxidation state of the atom, coordination, and the distances as well as coordination number and species of the atoms immediately surrounding the selected element. ATP binding is mediated by Mg^{2+}. However, probing Mg using XAS is technically difficult, and we therefore substituted Mn^{2+} for Mg^{2+}. Mn^{2+} is used extensively to substitute for the often spectroscopically silent Mg^{2+} because of the similarity of their properties,[26] including similar constants for binding to ATP.[27] In contrast to the NMR titration experiment in which ATP is the titrant, for X-ray absorption the concentration of Mn-ATP is constant. The absorption energy of Mn^{2+} as the cofactor of ATP was measured at increasing concentrations of eIF4G-HEAT1

dx.doi.org/10.1021/bi500600m | *Biochemistry* 2014, 53, 6422−6425

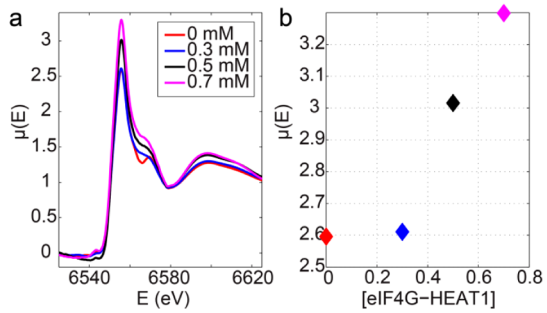

Figure 2. (a) Site-directed titration XANES analysis of the binding of eIF4G-HEAT1 to Mn-ATP. Each sample contained the same concentration of Mn-ATP (300 μM) and increasing concentrations of eIF4G-HEAT1: 0 mM (red), 0.3 mM (blue), 0.5 mM (black), and 0.7 mM (magenta). (b) Typical binding curve whereby each point in this curve represents the maximal amplitude value of each XANES spectrum vs ATP binding. Color coding as in panel a.

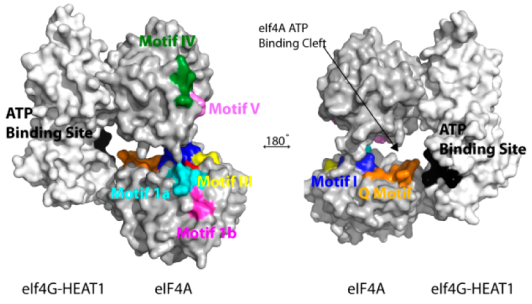

Figure 3. Mapping of the eIF4G-HEAT1 ATP binding site and helicase motifs on the model of the complex between eIF4G-HEAT1 and eIF4A. Helicase motifs are color coded using the system described in ref 30.

ranging from 0 to 0.7 mM. The energy profiles of these samples are shown in Figure 2a. Figure 2b shows the plot of the absorption edge versus eIF4G-HEAT1 concentration. The energy increases with increasing concentration, and the curve shows the characteristics of a typical binding curve. Binding is not saturated at 0.7 mM eIF4G-HEAT1; however, eIF4G-HEAT1 is not stable at higher concentrations. Together with the relatively small chemical shift changes and the inability to determine the binding constant with surface plasmon resonance (data not shown), this suggests that the binding site has a low affinity for ATP.

eIF4G-HEAT is known to bind to RNA.[28,29] Determination of the binding site of RNA [poly(U)] reveals that the binding sites for poly(U) and ATP do not overlap (see Figures S1−S3 of the Supporting Information). Although binding sites are distinct, binding of ATP to the eif4G-HEAT1 complex induces slight chemical shift changes for the residues involved in RNA binding. Chemical shifts for residues involved in ATP binding in these samples are slighlty different as well compared to those of the eIF4G-HEAT/ATP complex (see Figure S1 of the Supporting Information), which might suggest that RNA and ATP are able to bind to eIF4G-HEAT1 at the same time, but additional experiments would be needed to confirm this claim.

eIF4A is an ATP-dependent RNA helicase binding to eIF4G-HEAT1. The activity of eIF4A is enhanced by binding of eIF4G-HEAT1. The accepted mechanism for this enhancement was that in which eIF4G confers the closed, active conformation on eIF4A upon binding. We recently showed that the closed conformation of eIF4A is the preferred conformation in a crowded environment mimicking the cellular environment.[15] The ATPase activity of eIF4A is enhanced in a crowded environment without binding to eIF4G, which can be attributed to the conformational change. Binding of eIF4G-HEAT1 to eIF4A leads to an additional increase in activity.

Comparison of the structure of the complex in solution and in the crowded environment showed a compaction of the latter. Mapping the ATP binding site on eIF4GI-HEAT1 in a model of the eIF4GI-HEAT1/eIF4A complex reveals that the binding site is located right at the entrance to the binding cleft, opposite the ATP binding site on eIF4A (Figure 3).

The rate-limiting step in solution of the catalytic cycle of eIF4A was shown to be the release of phosphate after ATP hydrolysis.[31,32] This release is accelerated through interaction with eIF4G.[31] We showed previously that rate of ATP hydrolysis is increased in the presence of a crowding agent even without binding of eIF4G, which can be attributed to the fact that the crowded environment confers the closed, active conformation upon eIf4A.[15] However, an additional enhancement by binding of eIF4G to eIF4A is observed in a crowded environment, suggesting an additional reason for the activity enhancement. The additional enhancement of the activity of eIF4A by eIF4G could be explained by the presence of the ATP binding site on eIF4G-HEAT1. Binding of ATP in the proximity of the active site would not only increase the effective concentration of ATP but also reduce the entropy of the substrate by removing solvent molecules bound to ATP. However, additional experiments for studying this hypothesis would be needed.

■ ASSOCIATED CONTENT

Supporting Information

NMR spectra of eIF4G-HEAT titrations with ATP and RNA, chemical shift perturbation plots, and ATP and RNA epitope mapping on a model of eIF4G-HEAT1. This material is available free of charge via the Internet at http://pubs.acs.org.

■ AUTHOR INFORMATION

Corresponding Author

*E-mail: gerhard_wagner@hms.harvard.edu.

Funding

S.R.A. is funded by National Institutes of General Medical Sciences (NIGMS) Grant P01GM047467. G.W. thanks the National Cancer Institute (NCI) and NIGMS for funding this work: NCI Grant R01CA068262 and NIGMS Grant P01GM047467.

Notes

The authors declare no competing financial interest.

■ ACKNOWLEDGMENTS

Use of the National Synchrotron Light Source, Brookhaven National Laboratory, was supported by the U.S. Department of Energy, Office of Science, Office of Basic Energy Sciences, under Contract DE-AC02-98CH10886.

■ REFERENCES

(1) Kapp, L. D., and Lorsch, J. R. (2004) *Annu. Rev. Biochem.* 73, 657−704.

(2) Marintchev, A., and Wagner, G. (2004) *Q. Rev. Biophys.* 37, 197−284.

(3) Marintchev, A., Edmonds, K. A., Marintcheva, B., Hendrickson, E., Oberer, M., Suzuki, C., Herdy, B., Sonenberg, N., and Wagner, G. (2009) *Cell 136*, 447−460.
(4) Parsyan, A., Svitkin, Y., Shahbazian, D., Gkogkas, C., Lasko, P., Merrick, W. C., and Sonenberg, N. (2011) *Nat. Rev. Mol. Cell Biol. 12*, 235−245.
(5) Linder, P., Lasko, P. F., Ashburner, M., Leroy, P., Nielsen, P. J., Nishi, K., Schnier, J., and Slonimski, P. P. (1989) *Nature 337*, 121−122.
(6) Gorbalenya, A. E., and Koonin, E. V. (1993) *Curr. Opin. Struct. Biol. 3*, 419−429.
(7) Lorsch, J. R., and Herschlag, D. (1998) *Biochemistry 37*, 2180−2193.
(8) Pause, A., Methot, N., and Sonenberg, N. (1993) *Mol. Cell. Biol. 13*, 6789−6798.
(9) Grifo, J. A., Tahara, S. M., Leis, J. P., Morgan, M. A., Shatkin, A. J., and Merrick, W. C. (1982) *J. Biol. Chem. 257*, 5246−5252.
(10) Grifo, J. A., Abramson, R. D., Satler, C. A., and Merrick, W. C. (1984) *J. Biol. Chem. 259*, 8648−8654.
(11) Richter-Cook, N. J., Dever, T. E., Hensold, J. O., and Merrick, W. C. (1998) *J. Biol. Chem. 273*, 7579−7587.
(12) Abramson, R. D., Dever, T. E., Lawson, T. G., Ray, B. K., Thach, R. E., and Merrick, W. C. (1987) *J. Biol. Chem. 262*, 3826−3832.
(13) Korneeva, N. L., First, E. A., Benoit, C. A., and Rhoads, R. E. (2005) *J. Biol. Chem. 280*, 1872−1881.
(14) Oberer, M., Marintchev, A., and Wagner, G. (2005) *Genes Dev. 19*, 2212−2223.
(15) Akabayov, S. R., Akabayov, B., Richardson, C. C., and Wagner, G. (2013) *J. Am. Chem. Soc. 135*, 10040−10047.
(16) Marcotrigiano, J., Lomakin, I. B., Sonenberg, N., Pestova, T. V., Hellen, C. U., and Burley, S. K. (2001) *Mol. Cell 7*, 193−203.
(17) Caruthers, J. M., Johnson, E. R., and McKay, D. B. (2000) *Proc. Natl. Acad. Sci. U.S.A. 97*, 13080−13085.
(18) Chang, J. H., Cho, Y. H., Sohn, S. Y., Choi, J. M., Kim, A., Kim, Y. C., Jang, S. K., and Cho, Y. (2009) *Proc. Natl. Acad. Sci. U.S.A. 106*, 3148−3153.
(19) Schutz, P., Bumann, M., Oberholzer, A. E., Bieniossek, C., Trachsel, H., Altmann, M., and Baumann, U. (2008) *Proc. Natl. Acad. Sci. U.S.A. 105*, 9564−9569.
(20) Akabayov, S. R., and Wagner, G. (2014) *Biomol. NMR Assignments 8*, 89−91.
(21) Delaglio, F., Grzesiek, S., Vuister, G. W., Zhu, G., Pfeifer, J., and Bax, A. (1995) *J. Biomol. NMR 6*, 277−293.
(22) Johnson, B. A. (2004) *Methods Mol. Biol. 278*, 313−352.
(23) Akabayov, B., Lee, S. J., Akabayov, S. R., Rekhi, S., Zhu, B., and Richardson, C. C. (2009) *Biochemistry 48*, 1763−1773.
(24) Akabayov, B., and Richardson, C. C. (2011) *Powder Diffr. 26*, 159−162.
(25) Ravel, B., and Newville, M. (2005) *J. Synchrotron Radiat. 12*, 537−541.
(26) Reed, G. H., and Poyner, R. R. (2000) in *Metal ions in biological systems* (Sigel, H., Ed.) Vol. *37*, pp 183−207, Marcel Dekker Inc., New York.
(27) Sigel, H. (1987) *Eur. J. Biochem. 165*, 65−72.
(28) Pestova, T. V., and Hellen, C. U. (2003) *Cell 115*, 650−652.
(29) de Breyne, S., Yu, Y., Unbehaun, A., Pestova, T. V., and Hellen, C. U. (2009) *Proc. Natl. Acad. Sci. U.S.A. 106*, 9197−9202.
(30) Linder, P., and Lasko, P. (2006) *Cell 125*, 219−221.
(31) Hilbert, M., Kebbel, F., Gubaev, A., and Klostermeier, D. (2011) *Nucleic Acids Res. 39*, 2260−2270.
(32) Henn, A., Cao, W., Hackney, D. D., and De La Cruz, E. M. (2008) *J. Mol. Biol. 377*, 193−205.